ARTICLE

Activation of a novel α_{2A}AR-spinophilin-cofilin axis determines the effect of α_2 adrenergic drugs on fear memory reconsolidation

Shalini Saggu[1,2], Yunjia Chen[1], Christopher Cottingham[1,8], Hasibur Rehman[2], Hongxia Wang[1], Sixue Zhang[3], Corinne Augelli-Szafran[3,4], Sumin Lu[5], Nevin Lambert[5], Kai Jiao[6,7], Xin-Yun Lu[2] and Qin Wang[1,2]✉

Posttraumatic stress disorder (PTSD) after the pandemic has emerged as a major neuropsychiatric component of post-acute COVID-19 syndrome, yet the current pharmacotherapy for PTSD is limited. The use of adrenergic drugs to treat PTSD has been suggested; however, it is hindered by conflicting clinical results and a lack of mechanistic understanding of drug actions. Our studies, using both genetically modified mice and human induced pluripotent stem cell-derived neurons, reveal a novel α_{2A} adrenergic receptor (α_{2A}AR)-spinophilin-cofilin axis in the hippocampus that is critical for regulation of contextual fear memory reconsolidation. In addition, we have found that two α_2 ligands, clonidine and guanfacine, exhibit differential abilities in activating this signaling axis to disrupt fear memory reconsolidation. Stimulation of α_{2A}AR with clonidine, but not guanfacine, promotes the interaction of the actin binding protein cofilin with the receptor and with the dendritic spine scaffolding protein spinophilin to induce cofilin activation at the synapse. Spinophilin-dependent regulation of cofilin is required for clonidine-induced disruption of contextual fear memory reconsolidation. Our results inform the interpretation of differential clinical observations of these two drugs on PTSD and suggest that clonidine could provide immediate treatment for PTSD symptoms related to the current pandemic. Furthermore, our study indicates that modulation of dendritic spine morphology may represent an effective strategy for the development of new pharmacotherapies for PTSD.

Molecular Psychiatry (2023) 28:588–600; https://doi.org/10.1038/s41380-022-01851-w

INTRODUCTION

Posttraumatic stress disorder (PTSD) affects approximately 7–8% of the general population [1] and 11–20% of veterans [2] in the United States, when considering lifetime risk. The number of PTSD cases has further surged as a result of the COVID-19 pandemic; the prevalence of PTSD reaches over 30% both in patients who survived severe viral infection [3] and in frontline healthcare workers dealing with the pandemic [4]. Therefore, proper treatment of PTSD could have profound long-term impacts on human health and healthcare systems. However, currently there are only two FDA-approved medications for PTSD, and only 20–30% of patients achieve complete remission with treatment [5], indicating an urgent need to develop more effective pharmacotherapies for this mental illness.

The brain noradrenergic system plays an essential role in regulating emotional memory [6]. Noradrenergic dysfunction acts as a key contributing factor in the pathophysiology of PTSD [7], and the use of adrenergic ligands, including α_2 adrenergic receptor (AR) agonists, has been proposed as an attractive treatment for PTSD symptoms [8, 9]. Preclinical studies have demonstrated that pharmacological manipulations of α_2AR activities have profound impact on fear memory formation and retention [10–12], although the underlying molecular mechanism remains elusive. Importantly, multiple case reports and double-blinded clinical trials have demonstrated that clonidine, an α_2AR agonist, improves multiple symptoms associated with PTSD including nightmare, agitation, and poor sleep quality [13–19]. However, α_2-adrenergic modulation of PTSD-related processes has been challenged by clinical trials of another α_2AR agonist, guanfacine; in placebo-controlled trials, guanfacine fails to show significant efficacy for PTSD, arguing against the effectiveness of targeting α_2AR in PTSD treatment [20, 21]. The conflicting clinical effects and the lack of mechanistic understanding of drug actions have largely hindered the use of α_2AR agonists to treat PTSD. In this study, we attempt to resolve these conflicting clinical observations on α_2AR agonists by examining the mechanisms of action of these two drugs on fear memory using animal models and neurons derived from human induced pluripotent stem cells (hiPSCs).

[1]Department of Cell, Developmental and Integrative Biology, University of Alabama at Birmingham, Birmingham, AL 35294, USA. [2]Department of Neuroscience & Regenerative Medicine, Medical College of Georgia at Augusta University, Augusta, GA 30912, USA. [3]Department of Chemistry, Scientific Platforms, Southern Research, Birmingham, AL 35205, USA. [4]Scientific Platforms, Southern Research, Birmingham, AL 35205, USA. [5]Department of Pharmacology, Medical College of Georgia at Augusta University, Augusta, GA GA30912, USA. [6]Department of Genetics, University of Alabama at Birmingham, Birmingham, AL 35294, USA. [7]Center for Biotechnology and Genomic Medicine, Medical College of Georgia at Augusta University, Augusta, GA GA30912, USA. [8]Present address: Department of Biology, University of North Alabama, Florence, AL 35632, USA.
✉email: qin.wang@augusta.edu

Received: 19 May 2021 Revised: 12 October 2022 Accepted: 20 October 2022
Published online: 10 November 2022

Mounting evidence supports that previously stored memories can be reactivated by retrieval, entering a labile or destabilized state, and restabilized in an updated form [22–24]. This process is referred to as memory reconsolidation. Disruption of reconsolidation using pharmacological agents has been suggested as a promising therapeutic strategy for the treatment of PTSD [25]. Currently, a complete understanding of molecular mechanisms underlying memory reconsolidation is still lacking. Here we show, for the first time, that reconsolidation of fear memory requires dynamic changes in the activity and synaptic localization of cofilin.

Cofilin is an actin-severing protein and controls dendritic spine morphology and synaptic plasticity through regulating actin dynamics [26, 27]. Morphological changes of dendritic spines have been indicated as an essential cellular event that underlies learning and memory [28, 29] and disruption of these events is associated with many neuropsychiatric disorders including PTSD [30–32]. Activation of cofilin by dephosphorylation at Ser3 causes dendritic spine remodeling in hippocampal neurons, leading to transformation of mature mushroom-shaped spines into immature long thin spines [33]. Consistently, cofilin-deficient neurons show an increase in the number of mature neurons with large spine heads [34]. Changes in cofilin activity are required for both long-term potentiation (LTP) [35, 36] and long-term depression (LTD) [37, 38], the two key cellular/synaptic mechanisms for learning and memory. While cofilin inactivation leads to actin assembly and spine enlargement in LTP [35, 36], cofilin activation drives actin disassembly and spine shrinkage in LTD [37, 38]. Given the pivotal role of cofilin in these processes, precise regulation of its synaptic activity is essential to support proper actin reorganization in learning and memory. To date, our knowledge regarding the spatial and temporal control of cofilin activity during a physiological process, and how this can be manipulated by neurotransmitters and hormones as a means to regulate learning and memory, remains largely scarce. In the present study, we provide the first example that the spatial and temporal dynamics of cofilin at the synapse can be regulated by an FDA-approved adrenergic drug to modulate fear memory.

We identified cofilin as a novel downstream signaling effector that mediates α_{2A}AR-elicited regulation of fear memory reconsolidation. The two α_{2A}AR agonists, clonidine and guanfacine, show distinct ability in activating cofilin. Clonidine, but not guanfacine, promotes the interaction of cofilin with the receptor and with a synaptic scaffolding protein, spinophilin, which is essential in enhancing cofilin activity at the synapse. This ligand-selective activation of the α_{2A}AR-spinophilin-cofilin signaling axis leads to distinct regulation of contextual fear memory reconsolidation by clonidine and guanfacine and informs interpretation of differential clinical observations of these drugs on PTSD. Our study further suggests that pharmacological manipulation of spine morphology modulators such as cofilin represents an effective strategy for modification of fear memory reconsolidation, and thus has far-reaching implications for the development of active pharmacotherapies for PTSD.

MATERIALS AND METHODS

Animals

All experiments conformed to the National Institutes of Health Guide for the Care and Use of Laboratory Animals and were approved by the Institutional Animal Care and Use Committees (IACUC) of University of Alabama at Birmingham and Augusta University. Mice were maintained on a 12-h light/dark cycle with food and water continuously available and used at 3–5 months of age. α_{2A}AR deficient (*Adra2a*$^{-/-}$) were originally obtained from The Jackson Laboratory (stock number 004367) and bred and maintained on site at the C57BL/6 background. The generation of spinophilin deficient (*Ppp1r9b*$^{-/-}$) mice has been described previously [39], and the line has been backcrossed more than 10 generations to the C57BL/6 background. Both males and females were used, and we did not observe a significant difference between the sexes.

Reagents and antibodies

All peptides were synthesized and purified by GenScript, USA, Inc. Peptides containing a 16 aa sequence of the cofilin Ser3 site (MASGVAVSDGVIKVFN, referred to as S3 peptides) or phosphor-Ser3 site [MAS(p)GVAVSDGVIKVFN, referred to as pS3 peptides] were used. These peptides were fused to a TAT-like polyarginine membrane permeability sequence (GRRRRRRRRRR) to facilitate its entrance into cells and to a biotin molecule to allow detection. The TAT-like peptide (GRRRRRRRRRR) was used as a control. Antibodies to cofilin (cat #5175S, dilution 1:1000), phosphorylated cofilin (p-cofilin) (cat# 3311S, dilution 1:500) and Myc-Tag (9B11) (cat# #2276S, dilution 1:1000) were purchased from Cell Signaling Technology. HA.11 antibody (cat#901515) was from Biolegend. Clonidine (cat# C7897), guanfacine (cat#G1043), BRL44408 (cat# B4559) were from Sigma-Aldrich, and JP1302 (cat# 26-661-0) and imiloxan (cat# 09-861-0) were purchased from Thermo Fisher Scientific.

Cannulation and infusion of peptide

Stainless-steel bilateral guide cannulae (26 gauge, RWD Life Science, Inc) were implanted into the dorsal hippocampus (AP − 1.8 mm, ML ± 1.7, DV − 2.0), under isoflurane anesthesia, using standard stereotaxic procedures. Coordinates were chosen based on a mouse brain atlas. The cannula was anchored to the skull using screws and acrylic cement. The mice were allowed a recovery period of at least 1 week after surgery. The injection cannula was connected via PE Tubing (1.50*0.50 mm, RWD Life Science, Inc) to a 10 µl Hamilton micro syringe, driven by a microinjection pump (Dual Syringe, Model '11', Harvard apparatus, MA-70-2209). Infusions were administered in a volume of 1 µl over 5 min, and an additional 1 min was allowed for diffusion before the infusion cannulas were removed. Tat-S3, Tat-pS3 and Tat-control (100 µM, 1 µl, per side), were administered into the hippocampus immediately after re-exposure to conditioned stimuli.

Fear conditioning and test

For the fear conditioning paradigm, mice were placed into a standard fear-conditioning chamber (Coulbourn instruments, Habitest System). Mice were habituated to experimental chamber (Context A) for five minutes. On the next day (training day, TR), mice were placed into the same chamber (Context A) for 2 min and then received 2 sessions of tone-shock pairings (a tone for 30 s and an electric foot shock for 2 s at 0.5 mA) with an interval of 60 s between sessions. Following the presentation of the final stimulus, mice remained in the context for 60 s. Then 24 h later on reactivation day (RE), mice were first re-exposed to Context A for 3 min to test contextual fear memory. Mice were then moved to a novel context (Context B) and received 2 pairs of tones for 30 s without the shock to test cued fear memory. Saline, clonidine or guanfacine (0.5 mg/kg for both drugs) was injected intraperitoneally (i.p) immediately after re-exposure to both contextual and cued stimuli. 48 h (test session 1, TS1) and 96 h (test session 2, TS2) later, freezing behavior was measured and the percentage of freezing score was calculated as the percentage of time for which the mice remained immobile [40–44]. Heavy breathing, minimal movement and other movements required for normal respiration and autonomic function were considered as freezing behavior. Schematic presentation of the procedure is shown in Fig. 1A.

Preparation of hippocampal total lysates and the crude synaptosomal fraction

Hippocampi were dissected out and homogenized in a Dounce glass homogenizer with sucrose buffer (0.32 M sucrose, 4.2 mM Hepes buffer, pH7.4 with 0.1 mM $CaCl_2$, 1 mM $MgCl_2$ with protease and phosphatase inhibitors) and spun down at 1000 × *g* for 10 min at 4 °C. The supernatant (S1) fraction was collected, and one-fifth was used as total lysate and the remaining supernatant was centrifuged at 10,000 × *g* for 20 min at 4 °C. The resulting pellet containing the crude synaptosomal fraction was re-suspended in 1.5× lysis buffer (75 mM Tris, pH6.8, 15% Glycerol and 3% SDS), and protein concentration was quantified using a Bradford assay (Biorad) and protein concentrations were measured using the BioTek (Synergy 2) plate reader.

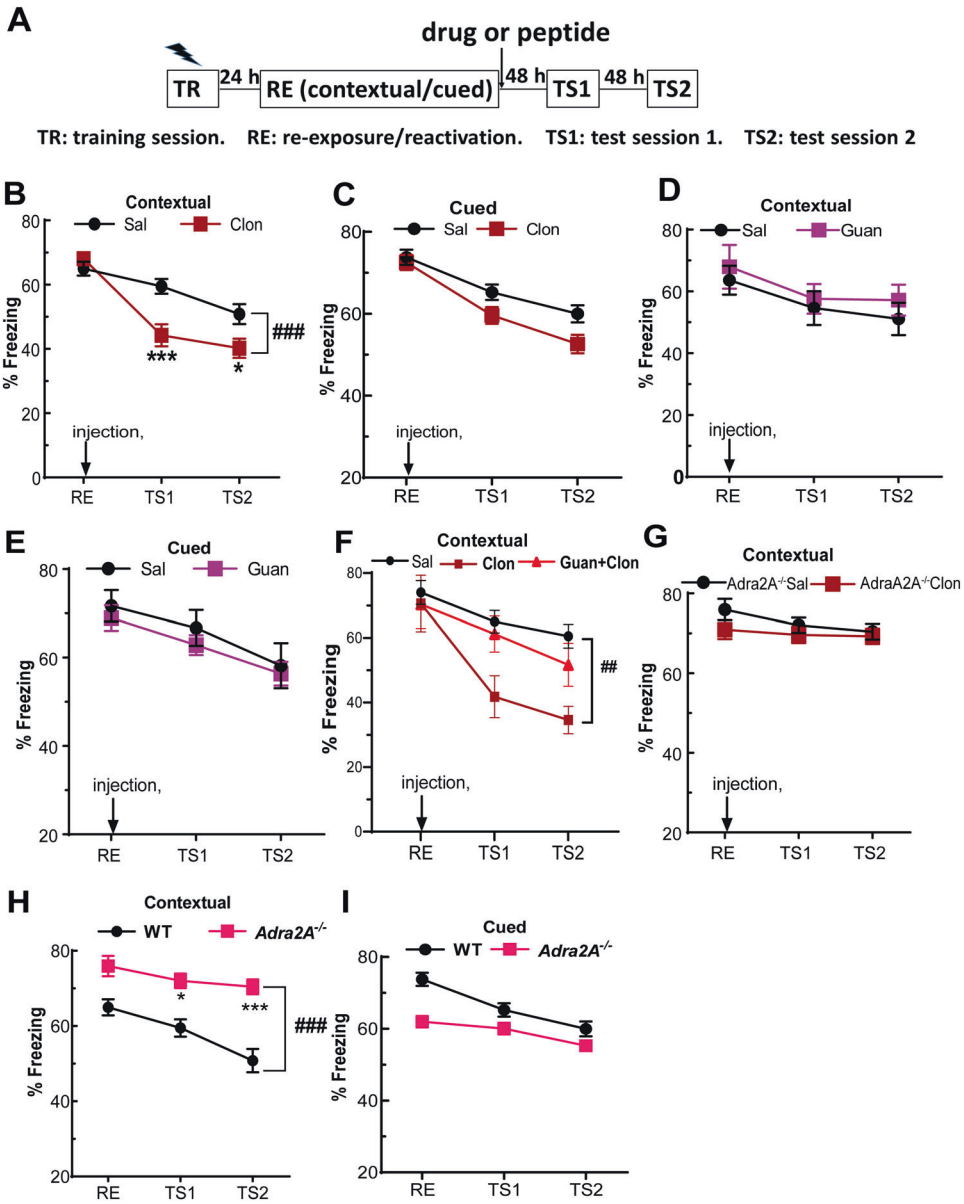

Fig. 1 Clonidine and guanfacine differentially regulate fear memory reconsolidation and cofilin activation through α_{2A}AR. A Schematic presentation of pavilion conditioning fear paradigm. The procedure is described in detail in Materials and Methods. Mice were injected interperitoneally (i.p.) with saline, clonidine (0.5 mg/kg) or guanfacine (0.5 mg/kg) immediately after re-exposure to contextual and cued stimuli. **B** Clonidine treatment immediately after fear memory reactivation (RE) reduces freezing to the context in test sessions (TS1 and TS2). The percentages of freezing time in response to the same context on indicated days are shown. $^{###}p < 0.001$, saline versus clonidine injected mice by two-way ANOVA; $^{*}p < 0.05$, $^{***}p < 0.001$, by Sidak's multiple comparisons test. $N = 14$ and 9 for the saline and clonidine group, respectively. **C** Clonidine shows no significant effect in the amount of freezing time induced by the conditioned cue in test sessions. Guanfacine treatment immediately after fear memory reactivation has no effect on freezing to the context (**D**) or cued (**E**) on test days. The percentages of freezing time are shown. $N = 6$/group. **F** Co-treatment with clonidine and guanfacine shows no significant effect on freezing to the context on test days. $^{##}p < 0.01$, saline versus clonidine by two-way ANOVA. $N = 8$ for saline, $n = 5$ for clonidine and $n = 6$ for clonidine +guanfacine. **G** Clonidine has no effect on freezing to the context in α_{2A}AR null (*Adra2a*$^{-/-}$) mice. $N = 6$/group. *Adra2A*$^{-/-}$ mice showed a stronger level of freezing in response to conditioned contextual (**H**), but not cued (**I**), stimuli on test days as compared to WT mice. $N = 14$ for WT and $n = 6$ for *Adra2A*$^{-/-}$ group. $^{###}p < 0.001$, *Adra2A*$^{-/-}$ versus WT mice by two-way ANOVA; $^{*}p < 0.05$, $^{***}p < 0.001$, versus WT by two-way ANOVA Sidak's multiple comparisons test. All data are expressed as mean ± SEM.

Cell culture and transfection

Neuro2A cells (ATCC, Cat# CCL-131) were cultured in 1:1 DMEM/Opti-MEM mix (Thermo Fisher Scientific) supplemented with 5% fetal bovine serum, 100 U/ml penicillin, and 100 µg/ml streptomycin. HEK293 cells (ATCC, Cat# CRL1573) were cultured in DMEM with 10% fetal bovine serum plus 100 U/ml penicillin, and 100 µg/ml streptomycin (Thermo Fisher Scientific). Cells were tested periodically for mycoplasma contamination.

Primary culture of hippocampal neurons was performed as described previously [45]. Briefly, newborn (postnatal day 0) mouse hippocampi were dissected out, minced, and digested with papain for 15 min at 37 °C. Neurons (2.5×10^4-1×10^5 cells/well) were plated in 24-well plates with Neurobasal-A medium supplemented with 5% FBS, 2% B27, 2% glutamax and 0.2% gentamycin. Feeding medium contained Neurobasal-A medium with 2% B27, 2% glutamax, 0.2% gentamycin. Neurons were treated after being cultured for 13–14 days in vitro (DIV).

Transfection of plasmids YFP-tagged cofilin^{WT} and cofilin^{S3D}, cofilin^{S3A} (Addgene) and myc tagged-spinophilin were performed using PureFection^{TM} transfection reagent (System Biosciences) according to manufacturer

instructions. 48 h post transfection, cells were stimulated with the appropriate ligands or vehicle.

Measurement of G protein coupling by the bioluminescence resonance energy transfer (BRET) assay

HEK 293 cells were transfected using linear polyethyleneimine MAX (PEI MAX; MW 40,000) at a nitrogen/phosphate ratio of 20 and were used for experiments 48 h later. Cells were transfected with α_{2A}AR-Rluc8, $G\alpha_{i1}$ or $G\alpha_{oA}$, Venus-1-155-$G\gamma_2$ and Venus-155-239-$G\beta_1$ in a (0.2:1:0.5:0.5) ratio for a total of 2.2 µg of plasmid DNA in each well of a 6-well plate. Cells were washed twice with permeabilization buffer (KPS) containing 140 mM KCl, 10 mM NaCl, 1 mM $MgCl_2$, 0.1 mM KEGTA, 20 mM NaHEPES (pH 7.2), harvested by trituration, permeabilized in KPS buffer containing 10 µg ml^{-1} high purity digitonin, and transferred to opaque black 96-well plates. Measurements were made from permeabilized cells supplemented with 2U ml^{-1} apyrase. BRET measurements were made using a Mithras LB940 photon-counting plate reader (Berthold Technologies GmbH, Bad Wildbad, Germany). Raw BRET signals were calculated as the emission intensity at 520–545 nm divided by the emission intensity at 475–495 nm.

Differentiation and culture of hiPSC-derived cortical neurons

Human iPSC-derived neural stem cells (NSCs, Axol #ax0018) were purchased from Axol Bioscience (UK). Donor information is readily available online (https://www.axolbio.com/). NSCs were cultured following Axol's enriched cerebral cortical neuron protocol to differentiate to cortical neurons. Briefly, 1×10^5 cells in neural plating medium (NPM) with 10 µM Y-27632 were seeded into each well of 24 well cell culture plate coated by 0.1 mg/ml PDL in ddH_2O and 1x SureBond-XF. On the next day (Day 1), NPM was replaced with neural differentiation medium (NDM) and changed on day 3 and day 5. On day 7, old media was discarded and complete neural maturation medium (CNMM) (Neurobasal A medium with 2% B-27 supplement, 1× GlutaMAX, 25uM2-Mercaptoethanol, 1x NeurOne Supplement B, 20 ng/mL BDNF, 0.5 mM cAMP and 0.2 mM Ascorbic Acid) was added to the plate and changed on day 9, 11 and 13. On day 15, CNMM was switched to neuronal culture medium (complete neural maturation medium without NeurOne Supplement B) followed by 50% medium change with neuronal culture medium every other day from Day 15. Stimulation was performed on Day 20. Lysates were prepared and subjected to Western blot.

Immunocytochemistry

Cells grown on coverslips were fixed with 4% paraformaldehyde at room temperature (RT) for 10 min and then permeabilized with 0.1% triton-X100 in PBS (PBST) for 30 min. Nonspecific binding was blocked by incubation in PBST with 5% goat serum for 60 min, following which mouse primary anti-α-tubulin (DSHB, E7, 1:200 dilution) antibody was applied overnight. After wash, anti-mouse Alexafluor488-conjugated secondary antibody was applied for 60 min at RT. F-actin was labeled by Alexafluor594-conjugated phalloidin (ThermoFisher). Images were obtained with NIKON A1R confocal microscope. Spine length and density was quantified using Image J (NIH).

Co-immunoprecipitation to detect protein-protein interaction

Co-immunoprecipitation was performed as described previously [46]. Briefly, HEK293T cells stably expressing HA-α_{2A}AR were transfected with $cofilin^{WT}$, pCAG-$cofilin^{S3D}$-YFP or pCAG-$cofilin^{S3A}$-YFP, together with Myc tagged-spinophilin. 48 h post transfection, cells were stimulated for 30 min and lysed in ice-cold immunoprecipitation (IP) buffer (10 mM Tris, 1% NP-40, 10% glycerol, 5 mM EDTA, and 5 mM EGTA, pH 7.6, plus protease inhibitors). Cell lysates were incubated with an anti-Myc or anti-spinophilin antibody overnight at 4 °C, followed by an additional 4-h incubation with 30 µl protein G bead slurry at 4 °C. For coimmunoisolation of endogenous spinophilin and cofilin from brain lysates, adult mice were treated with saline, clonidine or guanfacine through i.p. injection. 2 h post treatment, mouse brains were homogenized on ice in IP buffer described above. The detergent extract was then subjected to IP analyses with an anti-cofilin antibody.

Western blot

Cell and tissue lysates were resolved on SDS-PAGE and then transferred to a PVDF membrane (Biorad) followed by blocking with 5 % BSA in 1X Tris-buffered saline with 0.1% Tween-20 (TBST). The membrane was then incubated with proper primary antibody diluted in blocking buffer overnight at 4 °C. Next day, the membrane was extensively washed with TBST and incubated with a fluorescence- or HRP-conjugated secondary antibody. The membrane was scanned, and images were obtained using the LI-COR Odyssey system. The signal intensity was quantified using the Li-COR Image Studio software.

Fluorescence lifetime imaging microscopy (FLIM)-fluorescence resonance energy transfer (FRET) assay

Fluorescence lifetime imaging microscopy was used to study α_{2A}AR-spinophilin interaction in live cells as previously described [45]. Briefly, HEK293 cells plated onto 8-well micro slides were co-transfected with CFP-α_{2A}AR and YFP-spinophilin constructs. 48 h post transfection, cells were analyzed with an one-photon FLIM imaging system attached to a Zeiss LSM710 confocal microscope. FLIM-FRET efficiency (E) was calculated as: $E = 1$- (tFRET/tCFP), where tFRET and tCFP were the CFP lifetimes obtained for cells expressing CFP and YFP (unstimulated or stimulated prior to imaging) or CFP alone, respectively [45].

cAMP assay

The cAMP Hunter™ CHO-K1 ADRA2A-Gi cell line was purchased from Eurofins DiscoverX. Cells were seeded into white-walled 96-well tissue culture treated plates (5×10^4 cells/well). After 24 h, cells were stimulated with vehicle, clonidine or guanfacine, in the presence of 20 µM forskolin, for 30 min at 37 °C. Then cAMP levels were detected using HitHunter® cAMP assay kit (Eurofins DiscoverX) following manufacturer's manual. In brief, following stimulation in the cAMP assay buffer, antibody and the detection solution were added to each well and the assay plate was incubated at RT for 1 h in the dark. Next, cAMP Solution A was added to each well (including cAMP Standard wells) and the plate was incubated at RT for additional 3 h. Finally, luminescence intensity was measured using a BioTek Synergy H1 microplate reader.

β-arrestin assay

PathHunter CHO-K1 ADRA2A β-Arrestin Cell line (Eurofins # 93-0424C2) were seeded into a white-walled 96-well plate (100 µl, 2.5×10^4 cells/well). β-arrestin recruitment to activated α_{2A}AR was measured using PathHunter® Detection Kit (Eurofins #93-0001 M) following the manufacturer's instructions. Briefly, cells were stimulated with agonists or vehicle for 90 min at 37 °C followed by addition of working detection solution. After 1 h incubation at room temperature in the dark, luminescence intensity was measured using a BioTek Synergy H1 microplate reader.

Intact cell surface ELISA

Cell surface HA-A1R expression in primary neurons was examined by the cell-surface ELISA method as described previously [47, 48]. Primary hippocampal neurons were derived from HA-α_{2A}AR knock-in mice [49] and cultured for 14 days in vitro before tested. Neurons were stimulated, fixed, and then subjected to blocking, primary antibody (HA11, 1:3000), and secondary antibody (HRP-conjugated anti-mouse, 1:2000). Following incubation with o-phenylenediamine substrate (Pierce), absorbance at 490 nm was measured to determine surface HA-A1R density.

Statistical analysis

All statistical analyses were performed using GraphPad Prism 9.2.0.332 (GraphPad Software, San Diego). All groups for comparison were examined and analyzed in parallel for each experiment. The sample size for each experiment, including animal studies, was estimated based on similar experiments in previous studies [40–44, 47, 50–52]. For animal studies, mice were assigned randomly to different experimental groups, and investigators were blinded to the genotype or treatment during the experiments and when assessing the behavioral outcome, whenever possible. Data variation and normality were analyzed, and the variance was similar between groups that are being statistically compared. None of the samples were excluded from the analysis. Differences between two groups were compared for statistical significance by two-tailed unpaired Student's t-test. One-way and two-way ANOVA with *post hoc* multiple comparisons were applied when comparing multiple groups with one and two variables, respectively. $P < 0.05$ denotes significance. Data are expressed as means ± SE. Sample sizes, statistical tests used, and statistical results are indicated in the figure legends.

RESULTS

Clonidine and guanfacine show differential effects on fear memory reconsolidation and cofilin activation

To better understand the conflicting clinical effects of two α_2AR agonists, clonidine and guanfacine, on PTSD, we evaluated their effects on fear memory reconsolidation, following a Pavlovian fear conditioning procedure (Fig. 1A). Mice treated with clonidine immediately after re-exposed to the conditioned stimuli showed significantly less freezing time when tested in the same contextual environment than saline-treated mice in both test sessions, TS1 and TS2 (Fig. 1B). By contrast, guanfacine treatment had no effect on the freezing behavior (Fig. 1D). Furthermore, cotreatment with clonidine and guanfacine attenuated clonidine-induced disruption of fear memory reconsolidation (Fig. 1F). Neither clonidine nor guanfacine affected the amount of freezing time induced by the conditioned cue in test sessions (Fig. 1C, E). These data clearly demonstrate the distinct effects of clonidine and guanfacine on contextual fear memory reconsolidation; while clonidine effectively disrupts contextual fear memory, guanfacine acts as a competitive antagonist for this response.

α_{2A}AR is the primary α_2AR subtype expressed in the brain [53]. We next tested the role of this receptor subtype in clonidine-elicited impairment of contextual memory reconsolidation using mice lacking α_{2A}AR expression (*Adra2A*$^{-/-}$) [54]. Contrasting with observations in WT mice shown in Fig. 1B, clonidine treatment immediately after reactivation of fear memory had no effect on the freezing behavior in response to the conditioned context in the test sessions in α_{2A}AR deficient mice (Fig. 1G). Intriguingly, α_{2A}AR deficient mice showed a stronger level of freezing in response to conditioned contextual (Fig. 1H), but not cued (Fig. 1I), stimuli in test sessions when compared to WT mice. Consistently, treatment with a selective α_{2A} blocker, BRL44408, immediately after re-exposure resulted in an increased amount of freezing time in response to conditioned context on both test days (Supplementary Fig. S1). Conversely, ligands blocking the α_{2B} or α_{2C} receptor subtypes showed no significant effect on freezing behavior as compared to saline (Supplementary Fig. S1). Collectively, these data suggest that α_{2A}AR is a crucial regulator of contextual fear memory reconsolidation and mediates clonidine-elicited impairment of this process.

Clonidine and guanfacine share similar binding affinities at the α_{2A}AR [55]. To understand potential molecular mechanisms that could account for their distinct effects on contextual fear memory reconsolidation, we examined the abilities of these ligands to induce downstream signaling that can regulate learning and memory. We first tested two known α_{2A}AR downstream signaling effector cascades, cAMP inhibition and ERK1/2 activation. Clonidine and guanfacine exhibited similar efficacies in inhibiting cAMP levels (Supplementary Fig. S2A), and both effectively induced activation of ERK1/2 in primary neurons (Supplementary Fig. S2B). Given the importance of synaptic structures in learning and memory [28, 29] and the key role of cofilin in regulating dendritic spine dynamics [26, 27], we next asked whether cofilin can be activated downstream of α_{2A}AR and, if so, whether there is any difference between clonidine and guanfacine in inducing this signaling event. Cofilin activity is controlled by the phosphorylation status at Ser3; cofilin becomes inactive when it is phosphorylated at this residue [56]. Clonidine stimulation of Neuro2a cells led to a dose-dependent reduction of phospho-cofilin (at Ser3) levels compared to vehicle treatment (Fig. 2A and Supplementary Fig. S3), indicating activation of this protein by clonidine treatment. However, guanfacine stimulation failed to induce significant changes in cofilin phosphorylation (Fig. 2A, B). We further validated the differential effects of these two α_2AR agonists on cofilin activation in human neurons. As shown in Fig. 2C, D, in human iPSC-derived neurons, clonidine treatment, but not guanfacine treatment, led to a significant reduction in cofilin phosphorylation (Fig. 2C, D). We have therefore identified a novel signaling effector downstream of α_{2A}AR, namely cofilin, that can be activated by clonidine, but not by guanfacine.

Clonidine induces cofilin activation to regulate dendritic spine morphology in a spinophilin-dependent manner

Heterotrimeric G proteins and β arrestins are well-known signaling transducers of GPCRs. There is no significant difference between clonidine and guanfacine in inducing Gαi or Gαo association with α_{2A}AR (Supplementary Fig. S4). Both ligands also dose-dependently induced β-arrestin2 recruitment to the receptor (Supplementary Fig. S5A), an event critical for receptor internalization [48]. Consistently, clonidine and guanfacine induced a similar level of α_{2A}AR internalization in primary hippocampal neurons (Supplementary Fig. S5B). Our previous studies have revealed another key regulator of α_{2A}AR signaling and function, spinophilin [46, 57–60]. We found that clonidine, but not guanfacine, was able to drive rapid recruitment of spinophilin to the receptor in live cells (Fig. 2E and Supplementary Fig. S6). To determine whether spinophilin plays a role in clonidine-induced cofilin activation, we examined cofilin phosphorylation in primary hippocampal neurons derived from WT and spinophilin deficient (*Ppp1r9b*$^{-/-}$) mice. While clonidine treatment induced a time-dependent reduction of phospho-cofilin in WT neurons, it failed to do so in neurons lacking spinophilin (Fig. 2, F, G). Furthermore, in vivo treatment with clonidine significantly increased cofilin activity (indicated by the reduced phospho-cofilin level) in the hippocampus of WT, but not *Ppp1r9b*$^{-/-}$, mice (Fig. 2H, I). These data suggest that spinophilin is required for clonidine-induced cofilin activation.

Given the critical role of cofilin in regulating dendritic spine morphology [26, 27], we predicted that clonidine-induced cofilin activation would lead to morphological changes in dendritic spines. Indeed, in WT hippocampal neurons, clonidine treatment induced elongation of dendritic spines compared to vehicle treatment (Fig. 3A); the overall spine length (Fig. 3B) and the percentage of thin, long (>1.5 μm) spines (Fig. 3C) were significantly increased by clonidine treatment while spine densities were not changed (Fig. 3D). These clonidine-induced changes are similar to spine remodeling induced by cofilin activation [33]. Consistent with its requirement in clonidine-induced cofilin activation, spinophilin is also essential for clonidine-induced spine remodeling. In neurons without spinophilin expression (*Ppp1r9b*$^{-/-}$), clonidine failed to induce changes in spine morphology (Fig. 3A, B). In addition, there appeared to be a trend of increase in spine length in spinophilin-deficient neurons as compared to WT neurons under baseline conditions (Fig. 3B). Since guanfacine did not induce cofilin activation (Fig. 2A, B), we predicted that it would not alter spine morphology either. Indeed, guanfacine treatment failed to induce spine remodeling in WT hippocampal neurons (Supplementary Fig. S7).

To further validate that clonidine-induced changes in spine morphology rely on cofilin activation, we examined the effects of overexpression of wild type cofilin vs an inactive form of cofilin bearing the S3D mutation. While in hippocampal neurons with expression of wild type cofilin, clonidine treatment induces dendritic spine elongation compared to vehicle treatment, clonidine failed to do so when the cofilin-S3D mutant was overexpressed in neurons (Fig. 3E, F). Taken together, these data suggest that clonidine induces cofilin activation to regulate dendritic spine morphology in a spinophilin-dependent manner.

Spinophilin preferentially interacts with active cofilin and is required for maintaining cofilin activity and synaptic localization

Spinophilin is a scaffolding protein that contains a PDZ domain and the C-terminal end of cofilin possesses a PDZ-binding motif, although interaction between these two proteins has not been reported. Our co-immunoprecipitation (IP) assays revealed that the two proteins formed a complex in the mouse brain (Fig. 4A).

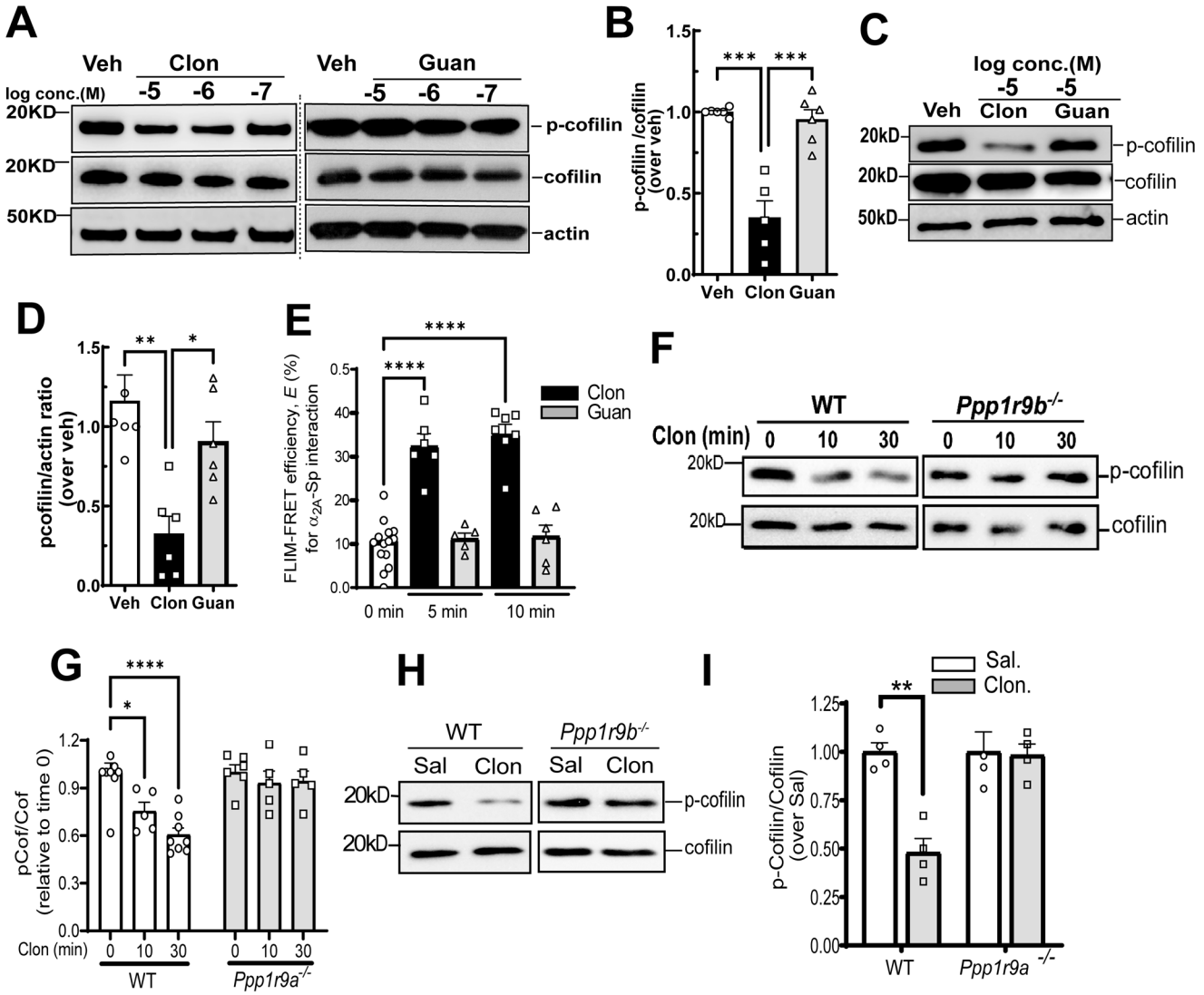

Fig. 2 Clonidine, but not guanfacine, induces cofilin activation in a spinophilin-dependent manner. A, **B** Neuro2A cells were stimulated with clonidine and guanfacine for 30 min and total cell lysates were subjected to Western blot analysis. Representative Western blots of phospho- (Ser3) and total cofilin (**A**) and quantification of the relative phospho- versus total cofilin ratio (**B**) are shown. ***$p < 0.001$ by one-way ANOVA Tukey's multiple comparisons test. $N = 5$ for clonidine group and $n = 6$ for vehicle and guanfacine group. **C**, **D** Human iPSC-derived neurons were stimulated with clonidine (10 μM) or guanfacine (10 μM) for 30 min. Representative Western blots (**C**) and quantification of the relative phospho- versus total cofilin ratio (**D**) are shown. *$p < 0.05$, **$p < 0.01$ by one-way ANOVA Tukey's multiple comparisons test. $N = 6$ per group. **E** Clonidine, but not guanfacine, induces spinophilin interaction with α_{2A}AR in live cells, as manifested by an increase in FLIM-FRET efficiency as compared to vehicle treatment. HEK293 cells stably expressing HAα_{2A}AR was stimulated with clonidine (10 μM) or guanfacine (10 μM) for indicated time. ****$p < 0.0001$ versus vehicle by one-way ANOVA Dunnett's multiple comparisons test. $N = 14$ for the 0-min time point; $n = 6$ and 5 for clonidine and guanfacine group, respectively, at the 5-min time point; $n = 7$ and 6 for clonidine and guanfacine group, respectively, at the 10-min time point. **F**, **G** Clonidine fails to induce cofilin activation in neurons lacking spinophilin expression. Primary hippocampal neurons derived from WT or *Ppp1r9b*$^{-/-}$ mice were treated with clonidine (10 μM) for the indicated times. Cell lysates were subjected to Western blot analysis to detect phospho- and total cofilin. Representative Western blots (**F**) and Quantification of the relative p-cofilin/cofilin ratio (**G**) are shown. *$p < 0.05$; ****$p < 0.0001$ by two-way ANOVA Tukey's multiple comparison test. For WT group, $n = 9$, 5 and 8 for the 0, 10 and 30-min time point, respectively; for *Ppp1r9b*$^{-/-}$ group, $n = 6$, 5 and 5 for the 0, 10 and 30-min time point, respectively. **H**, **I** Clonidine induces hippocampal cofilin activation in WT, but not *Ppp1r9b*$^{-/-}$, mice in vivo. Hippocampal lysates prepared from WT and *Ppp1r9b*$^{-/-}$ mice treated with saline or clonidine (0.5 mg/kg, i.p.) were subjected to Western blot analysis. Representative blots (**H**) and quantification of relative p-cofilin/cofilin ratio (**I**) are shown. **$p < 0.01$ by two-way ANOVA Tukey's multiple comparisons test. $N = 4$/group. All data are expressed as mean ± SEM.

We then asked whether changes in cofilin activity could affect its interaction with spinophilin. We examined spinophilin interaction with the constitutively active mutant form of cofilin, cofilin-S3A, and the inactive mutant of cofilin, cofilin-S3D, and detected a significantly higher level of cofilin-S3A than cofilin-S3D in the spinophilin-IP complex (Fig. 4B, C). The level of cofilin-S3A co-immunoisolated with spinophilin was nearly three-fold higher versus cofilin-S3D (Fig. 4C), suggesting that spinophilin preferentially interacts with active cofilin. We further determined whether spinophilin could regulate cofilin activity by examining the level of phospho-cofilin in the hippocampus of WT and *Ppp1r9b*$^{-/-}$ (spinophilin null) mice. In mice without spinophilin expression, the level of phospho-cofilin was significantly elevated as compared to that in WT mice (Fig. 4D, E), suggesting that spinophilin not only preferentially binds active cofilin but also is required for maintaining its activity in the hippocampus.

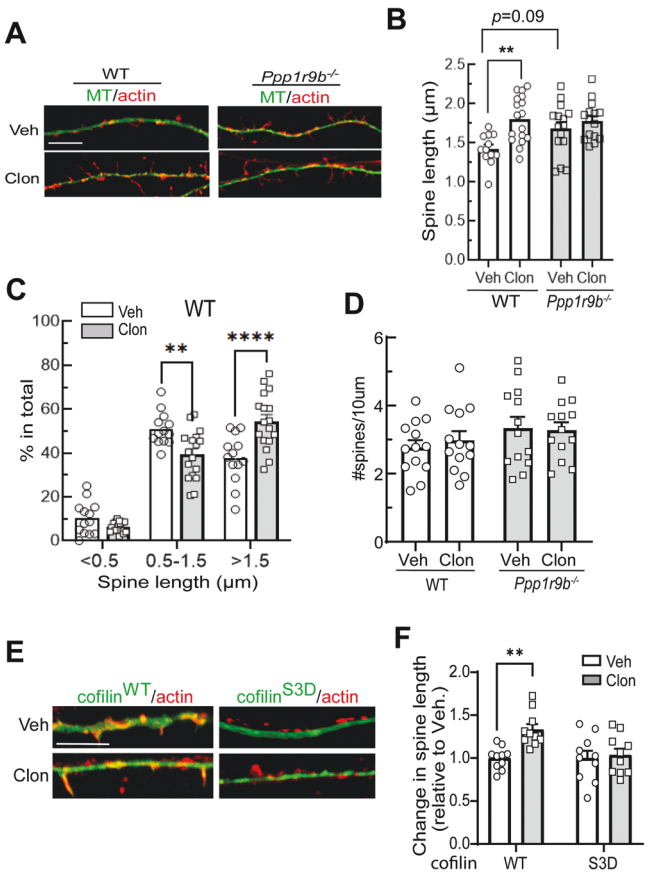

Fig. 3 Clonidine induces spine remodeling in a spinophilin- and cofilin-dependent manner. A–D Hippocampal neurons derived from WT or *Ppp1r9b*$^{-/-}$ mice were treated with vehicle (Veh) or clonidine (Clon, 10 μM) for 30 min, and stained for microtubule (MT, green) and actin (red). Representative images of dendritic spines are shown in **A**. Quantification of spine length (**B**), the percentages of spines at different lengths (**C**) and spine density (**D**) are also shown. $^{**}p < 0.01$; $^{****}p < 0.0001$ by two-way ANOVA Sidak's multiple comparisons test. For WT, $n = 12$ and 17 neurons for vehicle and clonidine, respectively, from four independent cultures. For *Ppp1r9b*$^{-/-}$, $n = 15$/group from four independent cultures. **E**, **F** Cofilin activation is required for clonidine-induced spine remodeling. Primary hippocampal neurons derived from WT mice were transfected with YFP-tagged cofilin WT or S3D mutant construct, treated with vehicle or clonidine (10 μM, 30 min) and stained for YFP-cofilin (WT or mutant, green) and actin (red). Representative images (**E**) and quantification (**F**) of spine length are shown. $^{**}p < 0.01$ by two-way ANOVA Sidak's multiple comparisons test. $N = 10$/group. All data are expressed as mean ± SEM.

Since spinophilin is enriched in dendritic spines [39, 61], we further examined whether interaction with spinophilin affects cofilin localization at the synapse using *Ppp1r9b*$^{-/-}$ (spinophilin null) mice. The level of cofilin in synaptosomes isolated from these mice was significantly reduced compared to that in synaptosomes from WT mice (Fig. 4G, H), whereas cofilin levels in the total hippocampal lysates were comparable between WT and spinophilin deficient mice (Fig. 4D, F). Taken together, our data suggest that spinophilin plays a crucial role in retaining active cofilin at the synapse.

The spinophilin-dependent cofilin dynamics at the synapse are required for fear memory reconsolidation

Although a role for cofilin in regulating learning and memory has been suggested [62], its activity and function in memory reconsolidation have not been addressed thoroughly. We first tested whether cofilin activity is changed during the fear memory reconsolidation process in the hippocampus, a brain region that is critical for encoding and maintaining contextual fear memory [43, 63]. We examined cofilin phosphorylation in the hippocampus at different time points after mice were re-exposed to conditioned stimuli. Phospho-cofilin (i.e., inactive cofilin) levels were significantly increased at both 0.5 and 2 h time points compared to the baseline level prior to re-exposure (Fig. 5A, B), suggesting that the memory reconsolidation process is accompanied by hippocampal cofilin inactivation.

To understand the importance of hippocampal cofilin activity in memory reconsolidation, we activated or inhibited cofilin using the cofilin S3 and pS3 peptide [64], respectively. TAT or TAT-fused S3 (TAT-S3) or pS3 (TAT-pS3) peptide was infused via bilateral intrahippocampal cannula immediately after mice were re-exposed to the conditioned stimuli (see Fig. 1A). Mice treated with the TAT-S3 peptide showed a reduced amount of freezing time in response to the conditioned context in test sessions when compared to mice treated with the TAT peptide or TAT-pS3 peptide (Fig. 5C). These data suggest that hippocampal cofilin inactivation is required for contextual fear memory reconsolidation; elevation of cofilin activity by the S3 peptide effectively disrupts this process. Consistent with the notion that the hippocampus is not involved in cued fear conditioning [65], hippocampal injection of the S3 peptide had no effect on freezing time in response to the conditioned cue in test sessions (Fig. 5D).

Concurrent with the change in cofilin activity during the reconsolidation process, we observed alterations in cofilin levels at the synapse. Reactivation of fear memory induced a significant reduction in cofilin levels in synaptosomes of the hippocampus at the 2-hr time point (Fig. 5E, F). Furthermore, this re-exposure-induced decrease in synaptic cofilin levels was gradually reversed on test days (Fig. 5H, I), correlated with gradually reduced memory strength on these days. Since spinophilin is important for the synaptic localization of cofilin, as revealed in Fig. 4, we next tested whether spinophilin plays a role in the synaptic dynamics of cofilin during fear memory reconsolidation. In mice lacking spinophilin expression, synaptic levels of cofilin were not altered after re-exposure to conditioned stimuli on any days tested (Fig. 5E, G, H), suggesting that spinophilin is required for the dynamic changes of cofilin at the synapse during fear memory reconsolidation.

Given the importance of spinophilin in regulating hippocampal cofilin dynamics revealed above, we predicted that spinophilin would play a role in contextual fear memory reconsolidation. Indeed, in *Ppp1r9b*$^{-/-}$ (spinophilin null) mice, the amount of freezing time in response to the conditioned context in test sessions was significantly increased as compared to WT mice (Fig. 5J), suggesting that the absence of spinophilin expression enhanced contextual fear memory reconsolidation in mice. The freezing on the reactivation day was comparable between *Ppp1r9b*$^{-/-}$ and WT mice (Fig. 5J), suggesting normal memory consolidation and retrieval in *Ppp1r9b*$^{-/-}$ mice. These data suggest that spinophilin is particularly important for regulating contextual fear memory reconsolidation while being dispensable for memory consolidation and retrieval. In mice without spinophilin expression, the reconsolidation process is enhanced, and fear memory persists despite repeated re-exposure to conditioned stimuli.

Clonidine, but not guanfacine, promotes the cofilin interaction with α_{2A}AR and spinophilin to disrupt contextual fear memory reconsolidation

Because of the essential role of synaptic cofilin dynamics in regulating fear memory reconsolidation as revealed above, to gain mechanistic insight into the differential regulation of contextual fear memory by clonidine and guanfacine, we tested the ability of these ligands to induce the interaction between α_{2A}AR and cofilin. Minimal interaction was detected between the two proteins under baseline conditions. In cells treated with clonidine, α_{2A}AR was readily co-immunoisolated with cofilin. However, guanfacine

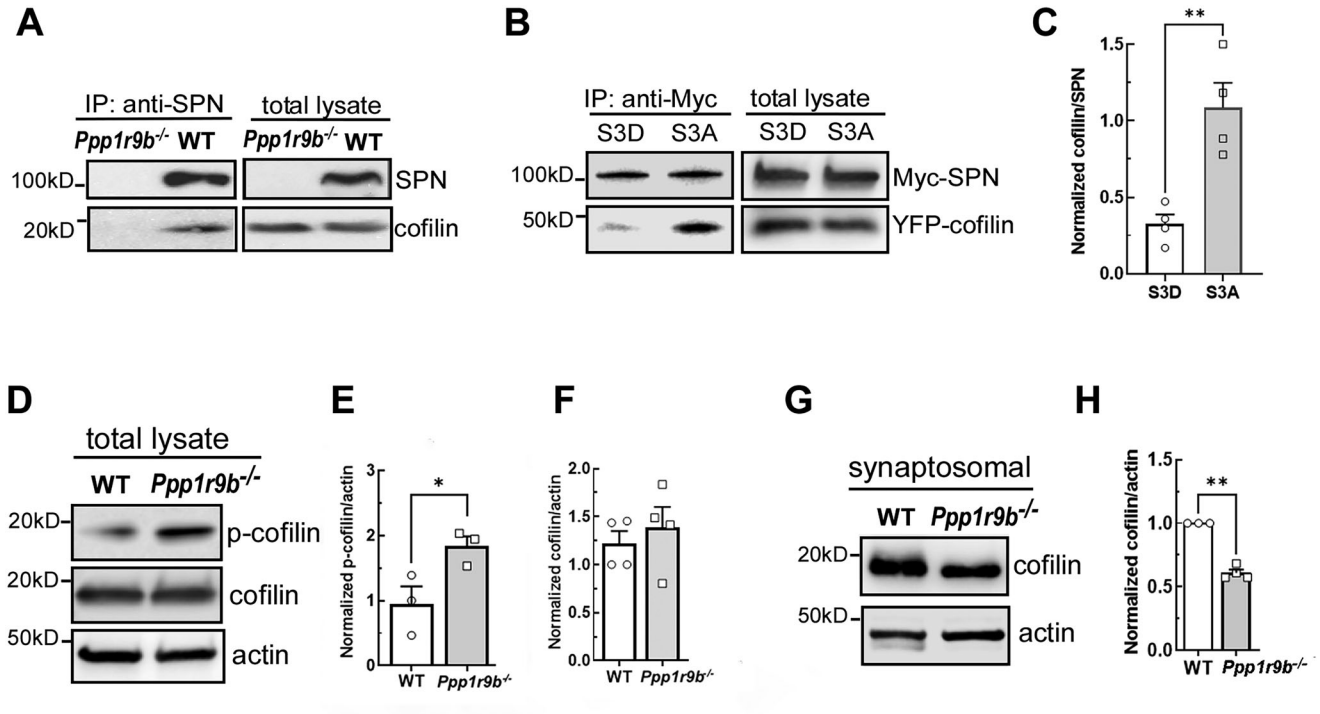

Fig. 4 Spinophilin preferentially interacts with active cofilin and retains cofilin at the synapse. A Spinophilin and cofilin form a complex in the mouse brain. Brain lysates prepared from WT or *Ppp1r9b*$^{-/-}$ mice were subjected to co-immunoprecipitation assays using a spinophilin antibody. Representative Western blots of spinophilin (SPN) and cofilin from multiple experiments are shown. **B**, **C** Spinophilin has a higher affinity to active cofilin compared to inactive cofilin. HEK293 cells were transfected with constructs of Myc-tagged spinophilin (Myc-SPN), together with either the constitutively active mutant cofilin (S3A) or inactive phosphomimetic cofilin (S3D) with an YFP tag. Cell lysates were immunoprecipitated with a Myc antibody. Representative Western blots (**B**) and quantification (**C**) of the relative level of each mutant cofilin in the spinophilin complex. $^{**}p < 0.01$, by Student's *t* test. $N = 4$/group. **D**–**F** The level of phospho-cofilin is increased (indicating lower cofilin activity) in *Ppp1r9b*$^{-/-}$mice as compared to WT mice. Hippocampal total lysates were blotted for phospho- and total cofilin. Representative blots (D) and quantification of phospho- (**E**) and total (**F**) cofilin. *, $p < 0.05$ versus WT by *t* test. $N = 3$/group in **E** and $n = 4$/group in **F**. **G**, **H** Less cofilin is detected in the synaptic fraction of the hippocampus in *Ppp1r9b*$^{-/-}$mice compared to WT mice. Representative Western blots (**G**) and quantifications of cofilin (**H**) in synaptosomal fractions of the hippocampus from WT and *Ppp1r9b*$^{-/-}$ mice. $^{**}p < 0.01$ vs. WT by *t* test. $N = 3$ for WT and $n = 4$ for *Ppp1r9b*$^{-/-}$. All data are expressed as mean ± SEM.

treatment failed to induce cofilin interaction with the receptor (Fig. 6A, B). Furthermore, the presence of guanfacine markedly reduced the level of α_{2A}AR-cofilin interaction induced by clonidine (Fig. 6C, D), suggesting that an antagonistic action of guanfacine in this process.

Clonidine treatment also significantly enhanced the interaction between cofilin and spinophilin in cells (Supplementary Fig. S8). Furthermore, in mice treated with clonidine in vivo, the level of spinophilin in complex with cofilin in the mouse hippocampus was significantly increased compared to saline treatment. By contrast, guanfacine treatment in vivo had no effect on the spinophilin-cofilin interaction (Fig. 6E, F). Taking these data together with the finding that clonidine stimulation increased the α_{2A}AR-spinophilin interaction (Fig. 2E), these data suggest that clonidine, but not guanfacine, promotes the complex formation among α_{2A}AR, spinophilin, and cofilin to facilitate cofilin activation.

We next investigated whether clonidine disrupts contextual memory reconsolidation through regulating cofilin dynamics during the process. As shown above in Fig. 5A, re-exposure to conditioned stimuli resulted in cofilin inactivation in the hippocampus. However, in mice receiving clonidine injection immediately after re-exposure to conditioned stimuli, the level of phospho-cofilin at the 2-hr time point was reduced to a level comparable to the basal level prior to re-exposure/reactivation (Fig. 6G, H), suggesting that clonidine treatment can efficiently prevent cofilin inactivation during fear memory reconsolidation. We then determined whether the change of cofilin activity is required for clonidine-elicited regulation of contextual fear memory reconsolidation. We infused, through bilateral intrahippocampal cannula, the TAT-pS3 peptide to block cofilin activation, or the TAT control peptide, immediately after mice were re-exposed to conditioned stimuli and injected with clonidine or saline. In mice receiving with the TAT peptide, clonidine treatment was able to reduce the freezing time in response to the conditioned context (Fig. 6I), consistent with our data shown in Fig. 1B. However, in mice infused with the TAT-pS3 peptide, clonidine failed to elicit changes in contextual fear memory reconsolidation (Fig. 6J). These data strongly suggest that clonidine-elicited disruption of contextual fear memory reconsolidation requires cofilin activation in the hippocampus.

Since clonidine induces cofilin activation in a spinophilin-dependent manner, we further determined the importance of spinophilin in clonidine-elicited regulation of contextual fear memory reconsolidation. As expected, contrasting with observations in WT mice (Fig. 1B), in spinophilin deficient mice, clonidine injection immediately after reactivation showed no effect on freezing behaviors in response to contextual stimuli in test sessions compared to saline injection (Fig. 6K). These data suggest that clonidine-induced effect on contextual fear memory reconsolidation requires the presence of spinophilin.

DISCUSSION

In the present study, we have identified a novel α_{2A}AR-spinophilin-cofilin axis in the hippocampus that is critical in regulating synaptic cofilin dynamics and contextual fear memory reconsolidation (SupplementaryFig. S9). Fear memory reconsolidation after

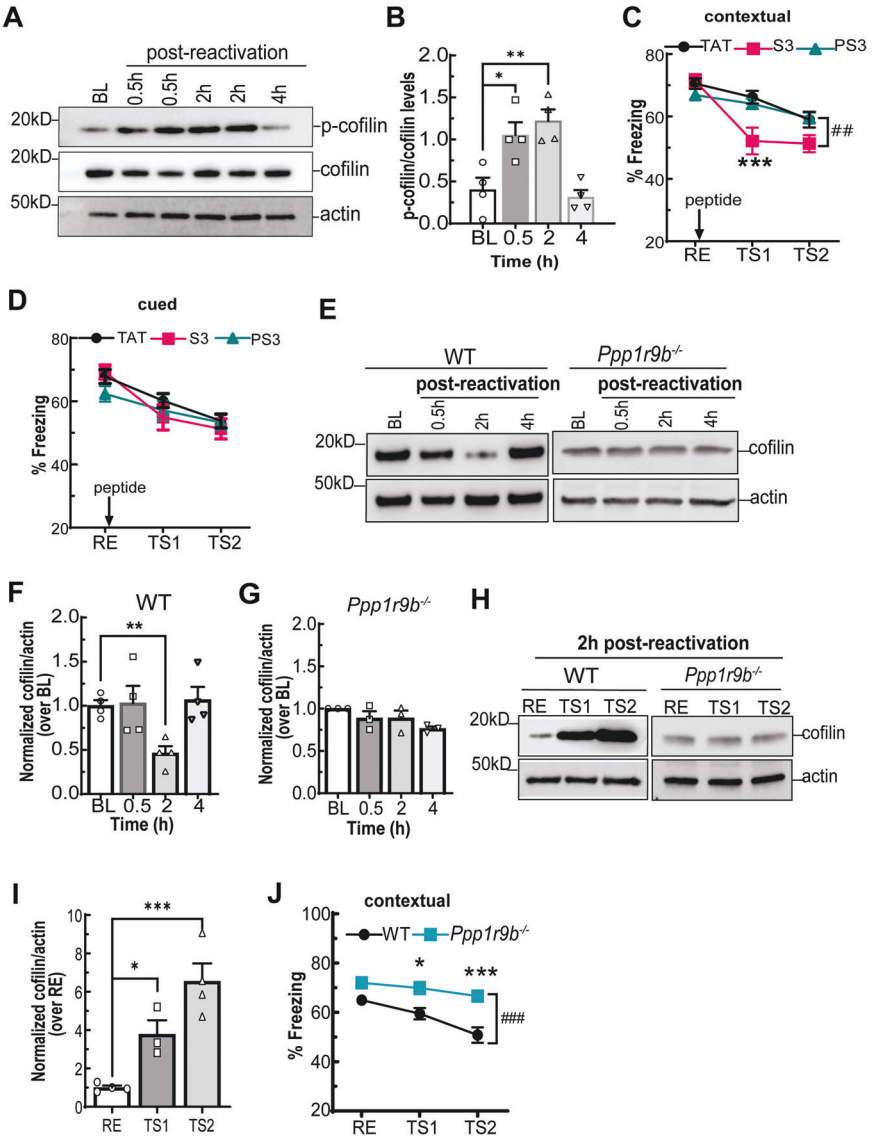

Fig. 5 Fear memory reconsolidation requires spinophilin-dependent changes in cofilin activity. A, **B** Fear memory reconsolidation is accompanied by changes in hippocampal cofilin phosphorylation. An increase in cofilin phosphorylation indicates reduction of cofilin activity. Representative immunoblots (**A**) of phospho-and total cofilin and actin at baseline (BL) prior to re-exposure to conditioned stimuli and at different time points after re-exposure are shown. Quantification of the relative phospho-cofilin/cofilin ratio is shown in **B**. $^{*}p < 0.05$; $^{**}p < 0.01$ versus BL by one-way ANOVA Tukey's multiple comparisons test. $N = 4$/group. **C** Hippocampal infusion of the cofilin S3 peptide disrupts contextual fear memory reconsolidation. TAT, TAT-S3, or TAT-pS3 peptide was microinfused bilaterally into the dorsal hippocampus immediately after re-exposure/reactivation. The percentage of freezing time in response to the same context on indicated days are shown. $N = 23$ for TAT, $n = 11$ for S3 and $n = 10$ for PS3 group. $^{\#\#}p < 0.01$, S3 versus TAT by two-way ANOVA. $^{***}p < 0.001$, S3 versus TAT by Sidak's multiple comparisons test. **D** Hippocampal infusion of the cofilin S3 peptide did not affect cued fear memory reconsolidation. **E**–**G** Reactivation induces a time-dependent reduction of synaptic cofilin levels in the hippocampus of WT, but not *Ppp1r9b*$^{-/-}$, mice. Synaptosomal fractions of the hippocampus were prepared at indicated time points after reactivation. BL, baseline prior to reactivation. Representative blots (**E**) and quantification (**F**, **G**) are shown. $^{**}p < 0.01$ versus BL by one-way ANOVA Tukey's multiple comparisons test. $N = 4$/group for WT in **F** and $n = 3$/group for *Ppp1r9b*$^{-/-}$ in **G**. **H**, **I** The level of synaptic cofilin at 2 h post re-exposure increases on test days, and this change requires spinophilin. Synaptosomal fractions of the hippocampus were prepared 2 h post re-exposure on indicated days. RE, TS1 and TS2 correspond to reactivation day, test day 1 and test day 2 as indicated in Fig. 1A. Representative blots (**H**) and quantification (**I**) are shown. $^{*}p < 0.05$; $^{***}p < 0.001$ by one-way ANOVA Tukey's multiple comparisons test. $N = 4$/group. **J** Enhanced freezing behavior in *Ppp1r9b*$^{-/-}$ mice on test days compared to WT mice in response to the conditioned context. $^{\#\#\#}p < 0.001$, versus WT by two-way ANOVA. $^{*}p < 0.05$; $^{***}p < 0.001$ by Sidak multiple comparisons test. $N = 15$ and 9 for WT and *Ppp1r9b*$^{-/-}$ mice, respectively. All data are expressed as mean ± SEM.

re-exposure to conditioned stimuli is accompanied by and requires a reduction in cofilin activity at the synapse. Stimulation of α_{2A}AR by clonidine, but not guanfacine, promotes the interaction of cofilin with α_{2A}AR and spinophilin to enhance the activity and synaptic localization of cofilin. When administered immediately after re-exposure to conditioned stimuli, clonidine, but not guanfacine, disrupts reconsolidation of contextual fear memory, and this effect relies on spinophilin-dependent cofilin activation (SupplementaryFig. S9). Our study thus uncovers a new molecular mechanism that regulates fear memory reconsolidation, which will facilitate future development of therapeutic strategies for emotional disorders such as PTSD.

Recent research has suggested that intervention of the reconsolidation process after retrieval/reactivation of previously

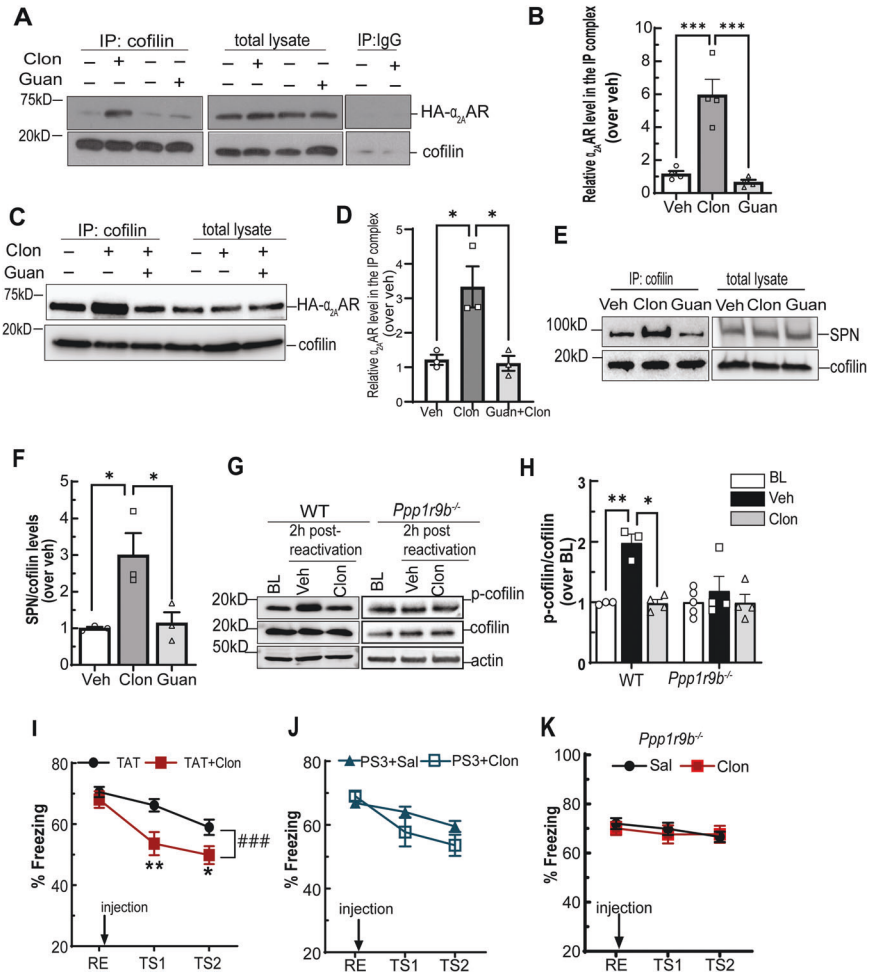

Fig. 6 Clonidine, but not guanfacine, promotes cofilin interaction with α_{2A}AR and spinophilin, and clonidine-elicited effects on contextual fear memory reconsolidation requires both cofilin and spinophilin. A, **B** Clonidine stimulation increases the complex formation between cofilin and α_{2A}AR. Neuro2A cells were stimulated with vehicle, clonidine (10 μM) or guanfacine (10 μM) for 30 min, and cell lysates were subjected to co-IP assays using a cofilin antibody. Representative blots (**A**) and quantification of the level of α_{2A}AR in the IP complex (**B**) are shown. ***$p < 0.001$ by one-way ANOVA Tukey's multiple comparisons test. $N = 4$/group. **C**, **D** The presence of guanfacine blocks clonidine-induced α_{2A}AR-cofilin interaction. Cells were stimulated with vehicle, clonidine or clonidine+guanfacine for 30 min, and cell lysates were subjected to co-IP assays using a cofilin antibody. Representative blots (**C**) and quantification of the level of α_{2A}AR in the IP complex (**D**) are shown. *$p < 0.05$ by one-way ANOVA Tukey's multiple comparisons test. $N = 3$/group. **E**, **F** Clonidine, but not guanfacine, treatment enhances the cofilin-spinophilin interaction in the mouse brain. Mice were injected i.p. with vehicle, clonidine (0.5 mg/kg) or guanfacine (0.5 mg/kg). 2 h post injection, hippocampal lysates were prepared and subjected to co-IP assays using a cofilin antibody. Representative blots (**E**) and quantification of the level of spinophilin in cofilin complex (**F**) are shown. *$p < 0.05$ versus vehicle by one-way ANOVA Tukey's multiple comparisons. $N = 3$/group. **G**, **H** Clonidine treatment prevents re-exposure-induced cofilin inactivation during the reconsolidation process. Clonidine (0.5 mg/kg) or saline was injected (i.p) immediately after re-exposure to conditioned stimuli. Representative Western blots (**G**) show the phospho- and total cofilin and actin at baseline (BL) prior to re-exposure and 2 h after re-exposure on reactivation day. Quantification of phospho-cofilin/cofilin levels over baseline is shown in **H**. *$p < 0.05$, **$p < 0.01$ by two-way ANOVA Tukey's multiple comparisons test. For WT, $n = 3$, 3 and 4 for baseline (BL), vehicle and clonidine group, respectively; for *Ppp1r9b*$^{-/-}$, $n = 5$, 4 and 4 for BL, vehicle and clonidine group. **I**, **J** Cofilin activation is required for clonidine-induced disruption of contextual fear memory reconsolidation. Immediately after re-exposure to contextual and cued stimuli, mice were infused bilaterally with TAT (**I**) or TAT-PS3 (**J**) peptide through intrahippocampal cannula and injected (i.p.) with saline or clonidine (0.5 mg/kg). $N = 22$ for TAT (with saline) and $n = 8$ for TAT-Clon group in **I**. ###$p < 0.001$, versus TAT group by two-way ANOVA; *$p < 0.05$, **$p < 0.01$, versus TAT by Sidak's multiple comparisons test. $N = 10$ and 9 for TAT-PS3 and TAT-PS3 + clonidine, respectively, in **J**. **K** Clonidine fails to alter contextual fear memory reconsolidation in *Ppp1r9b*$^{-/-}$ mice. Clonidine (0.5 mg/kg, i.p.) is administered immediately after reactivation. Freezing time is quantified in response to the conditioned context. All values are presented as mean ± SEM.

established memory can result in long-lasting modification of the memory [22–24]. Although changes in actin dynamics and dendritic spine morphology are well associated with learning and memory formation [66–69], evidence regarding whether and how dendritic spines are reshaped to facilitate the reconsolidation process remains largely elusive. We now show that reconsolidation of fear memory is accompanied by inactivation of an actin severing protein, cofilin, in the hippocampus, and this change is required for effective reconsolidation of contextual fear memory. Furthermore, reactivation of fear memory induces a significant reduction in synaptic localization of cofilin. Changes in cofilin activity and synaptic localization during reconsolidation are predicted to cause dendritic spine remodeling in this process, which warrants further investigation. Nonetheless, our study provides clear evidence suggesting modulators of actin dynamics as a promising target for modification of fear memory reconsolidation.

Despite the essential role of cofilin in regulating dendritic spine structure, information regarding mechanisms that regulate its

synaptic localization and retention remains limited. We identified that a dendritic spine-enriched scaffolding protein, spinophilin, plays a crucial role in regulating synaptic localization and activity of cofilin. Spinophilin is a multi-functional scaffolding protein highly enriched in dendritic spines [39, 61] and directly interacts with α_{2A}AR via the GPCR binding domain [70]. Here we found that spinophilin forms a complex with cofilin, presumably through its PDZ domain, which bind to the PDZ ligand motif at the C-terminal end of cofilin. Intriguingly, our data suggest that spinophilin preferentially interacts with the non-phosphorylated/active form cofilin. Furthermore, when spinophilin is absent, both cofilin activity and its synaptic localization are reduced in the hippocampus. Our data therefore support the notion that spinophilin interacts with active cofilin at the synapse to protect it from being phosphorylated/inactivated, thus serving as an important mechanism for retention of active cofilin at the synapse.

The spinophilin-dependent retention of cofilin is critical for the dynamic change of cofilin levels at the hippocampal synapse during the reconsolidation process; in spinophilin deficient mice, reactivation of fear memory failed to induce a reduction in synaptic cofilin levels in the hippocampus. Consequently, spinophilin deficient mice showed enhanced memory reconsolidation after each repeated reactivation with little extinction over time. On the other hand, loss of spinophilin has no effect on acquisition, consolidation and retrieval of fear memory, suggesting a specific role of spinophilin in regulating fear memory reconsolidation.

Although the α_{2A}AR has been well appreciated as an autoreceptor controlling NE release from adrenergic neurons, most of the central responses elicited by α_2AR ligands are in fact mediated by α_{2A}ARs expressed in non-adrenergic neurons [71]. For example, activation of postsynaptic α_{2A}AR in the prefrontal cortex enhances working memory through inhibiting HCN channels [72]. In another example, postsynaptic α_{2A}AR-mediated inhibition of HCN channels also enhances dorsal bed nucleus of the stria terminalis (BNST) neuronal activity to promote anxiogenic behaviors [73]. In our current study, we demonstrate, for the first time, that α_{2A}AR activation increases hippocampal cofilin activity through promoting complex formation between cofilin and spinophilin, and this α_{2A}AR-spinophilin-cofilin signaling axis is important for regulating the strength of contextual fear memory reconsolidation. When α_{2A}AR is blocked, genetically or pharmacologically, reconsolidation of contextual fear memory is enhanced, and little extinction is observed after repeated re-exposure to conditioned stimuli. By contrast, pharmacological blockade of the other two α_2AR subtypes, α_{2B} and α_{2C}, does not have a significant effect on contextual fear memory reconsolidation.

Both clonidine and guanfacine are clinically used α_{2A}AR agonists and share similar binding affinities to the receptor [49], and yet they show differential effects on PTSD symptoms. Consistent with the clinical observations, we observed distinct effects of clonidine and guanfacine on contextual fear memory reconsolidation; different from clonidine, guanfacine shows no effect on contextual fear memory reconsolidation. At the cellular level, clonidine, but not guanfacine, induces cofilin activation in a spinophilin-dependent fashion, even though both ligands effectively cause inhibition of cAMP and activation of ERK signaling, as well as receptor internalization. Furthermore, the presence of guanfacine blocks the α_{2A}AR-cofilin interaction induced by clonidine. Together, our data suggest that clonidine and guanfacine show distinct pharmacological properties at α_{2A}AR in engaging cofilin signaling; while clonidine acts as an agonist, guanfacine acts as a competitive antagonist. This clonidine action prevents cofilin inactivation during the reconsolidation process and thus reduces the strength of contextual fear memory reconsolidation. In further support of the notion that activation of the α_{2A}AR-spinophilin-cofilin signaling axis underlies clonidine-induced disruption of contextual fear memory reconsolidation, this clonidine-elicited response requires cofilin activation and the presence of spinophilin.

The phenomenon that clonidine and guanfacine selectively activate α_{2A}AR signaling pathways is referred to as ligand-selective agonism, a common feature observed for GPCRs and presumably caused by distinct structural conformations of the same receptor induced when in complex with different ligands [74–76]. Consistent with this notion, our in-silico docking studies suggest differences in residual-interaction patterns between clonidine and guanfacine binding to α_{2A}AR. Despite both ligands binding to the same site and forming a salt-bridge/hydrogen bond with residue D113 of α_{2A}AR, the basic head of guanfacine displays a different binding pattern than the imidazole head of clonidine and forms two additional hydrogen bonds with E189 (Supplementary Fig. S10). E189 is a key orthostatic residue and part of an interaction network regulating ligand binding [77], and an α_{2A}AR antagonist, yohimbine, is predicted to form H-bond with E189 [78]. Our experimental evidence indeed suggests antagonistic features of guanfacine in blocking clonidine-induced α_{2A}AR cofilin interaction and in attenuating clonidine-induced disruption of fear memory reconsolidation. Intriguingly, the predicted difference in receptor binding between clonidine and guanfacine does not cause distinction in G protein coupling or arrestin interaction with α_{2A}AR. However, it sufficiently leads to differential complex formation of the receptor with spinophilin and cofilin, suggesting a higher sensitivity of spinophilin-mediated signaling to conformational changes in α_{2A}AR. Thus, in addition to G proteins and arrestins, spinophilin can act as effective mediator of GPCR ligand-biased signaling.

Our current study has strong clinical implications. Following global pandemics, including COVID-19, PTSD can affect over 20% of all populations, with even stronger effects on infected patients and frontline health workers [4]. The dearth of effective FDA-approved treatments has driven off-label usage of other medications, including adrenergic ligands, for PTSD treatment. Effectively repurposing existing medications for the immediate treatment of PTSD requires a better understanding of molecular and cellular mechanisms underlying drug actions. Our current study reveals a novel α_{2A}AR-spinophilin-cofilin signaling axis that regulates contextual fear memory reconsolidation and distinguishes the efficacies of α_{2A}AR agonists in disrupting this process. Our observation of no effect of guanfacine on fear memory reconsolidation in mice could help interpret the failure of double-blinded, placebo-controlled clinical trials with this agonist [20, 21]. On the other hand, our data support the usefulness of clonidine in treating PTSD. Although no large placebo-controlled trials have been conducted for clonidine, its usage has been observed to be effective in multiple clinical practice and trials [13–19]. Large scale, placebo-controlled clinical trials for clonidine in PTSD are warranted. If successful, clonidine would provide immediate treatment to PTSD in general populations and veterans and help combat the mental health issues associated with the COVID-19 pandemic. Furthermore, cofilin activation could provide an effective screening tool for selecting other α_{2A}AR ligands or pharmacotherapeutic agents for PTSD treatment. Our study thus has far-reaching implications for the development of active pharmacotherapies for PTSD.

REFERENCES

1. Kessler RC, Sonnega A, Bromet E, Hughes M, Nelson CB. Posttraumatic stress disorder in the National Comorbidity Survey. Arch Gen Psychiatry. 1995;52:1048–60.
2. Group TMoP-TSW. VA/DoD clinical practice guideline: management of posttraumatic stress. In: Defense DoVAaDo (ed). Washington, D.C.: U.S. Department of Veterans Affairs; 2010.
3. Janiri D, Carfì A, Kotzalidis GD, Bernabei R, Landi F, Sani G, et al. Posttraumatic Stress Disorder in Patients After Severe COVID-19 Infection. JAMA Psychiatry. 2021;78:567–9.
4. Yuan K, Gong YM, Liu L, Sun YK, Tian SS, Wang YJ, et al. Prevalence of posttraumatic stress disorder after infectious disease pandemics in the twenty-first century, including COVID-19: a meta-analysis and systematic review. Mol Psychiatry. 2021; 26:4982–98.

5. Berger W, Mendlowicz MV, Marques-Portella C, Kinrys G, Fontenelle LF, Marmar CR, et al. Pharmacologic alternatives to antidepressants in posttraumatic stress disorder: a systematic review. Prog Neuro Psychopharmacol Biol psychiatry. 2009;33:169–80.
6. van Stegeren AH. The role of the noradrenergic system in emotional memory. Acta Psychol (Amst). 2008;127:532–41.
7. Hendrickson RC, Raskind MA. Noradrenergic dysregulation in the pathophysiology of PTSD. Exp Neurol. 2016;284:181–95. Pt B
8. Belkin MR, Schwartz TL. Alpha-2 receptor agonists for the treatment of posttraumatic stress disorder. Drugs Context. 2015;4:212286.
9. Lakhkar A. Adrenergic receptor agonists and antagonists in the treatment of post traumatic stress disorder. Munich: GRIN Verlag; 2010.
10. Gamache K, Pitman RK, Nader K. Preclinical evaluation of reconsolidation blockade by clonidine as a potential novel treatment for posttraumatic stress disorder. Neuropsychopharmacology. 2012;37:2789–96.
11. Gazarini L, Stern CA, Carobrez AP, Bertoglio LJ. Enhanced noradrenergic activity potentiates fear memory consolidation and reconsolidation by differentially recruiting alpha1- and beta-adrenergic receptors. Learn Mem. 2013;20:210–9.
12. Holmes NM, Crane JW, Tang M, Fam J, Westbrook RF, Delaney AJ. alpha2-adrenoceptor-mediated inhibition in the central amygdala blocks fear-conditioning. Sci Rep. 2017;7:11712.
13. Kinzie JD, Leung P. Clonidine in Cambodian patients with posttraumatic stress disorder. J Nerv Ment Dis. 1989;177:546–50.
14. Porter DM, Bell CC. The use of clonidine in post-traumatic stress disorder. J Natl Med Assoc. 1999;91:475–7.
15. Alao A, Selvarajah J, Razi S. The use of clonidine in the treatment of nightmares among patients with co-morbid PTSD and traumatic brain injury. Int J Psychiatry Med. 2012;44:165–9.
16. Wendell KR, Maxwell ML. Evaluation of Clonidine and Prazosin for the Treatment of Nighttime Posttraumatic Stress Disorder Symptoms. Fed Pr. 2015;32:8–14.
17. Kinzie JD, Sack RL, Riley CM. The polysomnographic effects of clonidine on sleep disorders in posttraumatic stress disorder: a pilot study with Cambodian patients. J Nerv Ment Dis. 1994;182:585–7.
18. Ziegenhorn AA, Roepke S, Schommer NC, Merkl A, Danker-Hopfe H, Perschel FH, et al. Clonidine improves hyperarousal in borderline personality disorder with or without comorbid posttraumatic stress disorder: a randomized, double-blind, placebo-controlled trial. J Clin Psychopharmacol. 2009;29:170–3.
19. Mousavi S, Barati M, Afshar H, Bashardoust N. The comparison between prazosin versus clonidine effects on combat related P.T.S.D nightmares. Ann Gen Psychiatry. 2006;5:S190.
20. Neylan TC, Lenoci M, Samuelson KW, Metzler TJ, Henn-Haase C, Hierholzer RW, et al. No improvement of posttraumatic stress disorder symptoms with guanfacine treatment. Am J psychiatry. 2006;163:2186–8.
21. Davis LL, Ward C, Rasmusson A, Newell JM, Frazier E, Southwick SM. A placebo-controlled trial of guanfacine for the treatment of posttraumatic stress disorder in veterans. Psychopharmacol Bull. 2008;41:8–18.
22. Lee JL. Reconsolidation: maintaining memory relevance. Trends Neurosci. 2009;32:413–20.
23. Exton-McGuinness MT, Lee JL, Reichelt AC. Updating memories-the role of prediction errors in memory reconsolidation. Behav Brain Res. 2015;278:375–84.
24. Tronson NC, Taylor JR. Molecular mechanisms of memory reconsolidation. Nat Rev Neurosci. 2007;8:262–75.
25. Beckers T, Kindt M. Memory Reconsolidation Interference as an Emerging Treatment for Emotional Disorders: Strengths, Limitations, Challenges, and Opportunities. Annu Rev Clin Psychol. 2017;13:99–121.
26. Hild G, Kalmar L, Kardos R, Nyitrai M, Bugyi B. The other side of the coin: functional and structural versatility of ADF/cofilins. Eur J Cell Biol. 2014;93:238–51.
27. Rust MB. ADF/cofilin: a crucial regulator of synapse physiology and behavior. Cell Mol Life Sci. 2015;72:3521–9.
28. Yuste R, Bonhoeffer T. Morphological changes in dendritic spines associated with long-term synaptic plasticity. Annu Rev Neurosci. 2001;24:1071–89.
29. Caroni P, Donato F, Muller D. Structural plasticity upon learning: regulation and functions. Nat Rev Neurosci. 2012;13:478–90.
30. Fiala JC, Spacek J, Harris KM. Dendritic spine pathology: cause or consequence of neurological disorders? Brain Res Brain Res Rev. 2002;39:29–54.
31. Penzes P, Cahill ME, Jones KA, VanLeeuwen JE, Woolfrey KM. Dendritic spine pathology in neuropsychiatric disorders. Nat Neurosci. 2011;14:285–93.
32. Blanpied TA, Ehlers MD. Microanatomy of dendritic spines: emerging principles of synaptic pathology in psychiatric and neurological disease. Biol psychiatry. 2004; 55:1121–7.
33. Shi Y, Pontrello CG, DeFea KA, Reichardt LF, Ethell IM. Focal adhesion kinase acts downstream of EphB receptors to maintain mature dendritic spines by regulating cofilin activity. J Neurosci. 2009;29:8129–42.
34. Rust MB, Gurniak CB, Renner M, Vara H, Morando L, Gorlich A, et al. Learning, AMPA receptor mobility and synaptic plasticity depend on n-cofilin-mediated actin dynamics. Embo J. 2010;29:1889–902.
35. Chen LY, Rex CS, Casale MS, Gall CM, Lynch G. Changes in synaptic morphology accompany actin signaling during LTP. J Neurosci. 2007;27:5363–72.
36. Bosch M, Castro J, Saneyoshi T, Matsuno H, Sur M, Hayashi Y. Structural and molecular remodeling of dendritic spine substructures during long-term potentiation. Neuron. 2014;82:444–59.
37. Zhou Z, Hu J, Passafaro M, Xie W, Jia Z. GluA2 (GluR2) regulates metabotropic glutamate receptor-dependent long-term depression through N-cadherin-dependent and cofilin-mediated actin reorganization. J Neurosci. 2011;31:819–33.
38. Pontrello CG, Sun MY, Lin A, Fiacco TA, DeFea KA, Ethell IM. Cofilin under control of beta-arrestin-2 in NMDA-dependent dendritic spine plasticity, long-term depression (LTD), and learning. Proc Natl Acad Sci USA. 2012;109:E442–451.
39. Feng J, Yan Z, Ferreira A, Tomizawa K, Liauw JA, Zhuo M, et al. Spinophilin regulates the formation and function of dendritic spines. Proc Natl Acad Sci USA. 2000;97:9287–92.
40. Suzuki A, Josselyn SA, Frankland PW, Masushige S, Silva AJ, Kida S. Memory reconsolidation and extinction have distinct temporal and biochemical signatures. J Neurosci. 2004;24:4787–95.
41. Lugo JN, Smith GD, Holley AJ. Trace fear conditioning in mice. J Vis Exp. 2014; 85:51180.
42. Shoji H, Takao K, Hattori S, Miyakawa T. Contextual and cued fear conditioning test using a video analyzing system in mice. J Vis Exp. 2014;85:50871
43. Kim WB, Cho JH. Encoding of contextual fear memory in hippocampal-amygdala circuit. Nat Commun. 2020;11:1382.
44. Balogh SA, Radcliffe RA, Logue SF, Wehner JM. Contextual and cued fear conditioning in C57BL/6J and DBA/2J mice: context discrimination and the effects of retention interval. Behav Neurosci. 2002;116:947–57.
45. Cottingham C, Chen Y, Jiao K, Wang Q. The Antidepressant Desipramine Is an Arrestin-biased Ligand at the {alpha}2A-Adrenergic Receptor Driving Receptor Down-regulation in Vitro and in Vivo. JBiolChem. 2011;286:36063–75.
46. Xu J, Chen Y, Lu R, Cottingham C, Jiao K, Wang Q. Protein kinase A phosphorylation of spinophilin modulates its interaction with the alpha 2A-adrenergic receptor (AR) and alters temporal properties of alpha 2AAR internalization. J Biol Chem. 2008;283:14516–23.
47. Chen Y, Liu Y, Cottingham C, McMahon L, Jiao K, Greengard P, et al. Neurabin scaffolding of adenosine receptor and RGS4 regulates anti-seizure effect of endogenous adenosine. J Neurosci. 2012;32:2683–95.
48. Cottingham C, Chen Y, Jiao K, Wang Q. The antidepressant desipramine is an arrestin-biased ligand at the alpha(2A)-adrenergic receptor driving receptor down-regulation in vitro and in vivo. J Biol Chem. 2011;286:36063–75.
49. Lu R, Li Y, Zhang Y, Chen Y, Shields AD, Winder DG, et al. Epitope-tagged receptor knock-in mice reveal that differential desensitization of alpha2-adrenergic responses is because of ligand-selective internalization. J Biol Chem. 2009;284:13233–43.
50. Zhang F, Gannon M, Chen Y, Yan S, Zhang S, Feng W, et al. beta-amyloid redirects norepinephrine signaling to activate the pathogenic GSK3beta/tau cascade. Sci Transl Med. 2020;12:eaay6931.
51. Zhang F, Gannon M, Chen Y, Zhou L, Jiao K, Wang Q. The amyloid precursor protein modulates alpha2A-adrenergic receptor endocytosis and signaling through disrupting arrestin 3 recruitment. FASEB J. 2017;31:4434–46.
52. Cottingham C, Lu R, Jiao K, Wang Q. Cross-talk from beta-adrenergic receptors modulates alpha2A-adrenergic receptor endocytosis in sympathetic neurons via protein kinase A and spinophilin. J Biol Chem. 2013;288:29193–205.
53. Bucheler MM, Hadamek K, Hein L. Two alpha(2)-adrenergic receptor subtypes, alpha(2A) and alpha(2C), inhibit transmitter release in the brain of gene-targeted mice. Neuroscience. 2002;109:819–26.
54. Altman JD, Trendelenburg AU, MacMillan L, Bernstein D, Limbird L, Starke K, et al. Abnormal regulation of the sympathetic nervous system in alpha2A- adrenergic receptor knockout mice. MolPharmacol. 1999;56:154–61.
55. Lu R, Li Y, Zhang Y, Chen Y, Shields AD, Winder DG, et al. Epitope-tagged Receptor Knock-in Mice Reveal That Differential Desensitization of {alpha}2-Adrenergic Responses Is because of Ligand-selective Internalization. JBiolChem. 2009;284:13233–43.
56. Yang N, Higuchi O, Ohashi K, Nagata K, Wada A, Kangawa K, et al. Cofilin phosphorylation by LIM-kinase 1 and its role in Rac-mediated actin reorganization. Nature 1998;393:809–12.
57. Wang Q, Zhao J, Brady AE, Feng J, Allen PB, Lefkowitz RJ, et al. Spinophilin blocks arrestin actions in vitro and in vivo at G protein-coupled receptors. Science. 2004;304:1940–4.
58. Cottingham C, Lu R, Jiao K, Wang Q. Cross-talk from beta adrenergic receptors modulates alpha$_{2A}$ adrenergic receptor endocytosis in sympathetic neurons via protein kinase A and spinophilin. J Biol Chem. 2013;288:29193–205.
59. Cottingham C, Li X, Wang Q. Noradrenergic antidepressant responses to desipramine in vivo are reciprocally regulated by arrestin3 and spinophilin. Neuropharmacology. 2012;62:2354–62.
60. Lu R, Chen Y, Cottingham C, Peng N, Jiao K, Limbird LE, et al. Enhanced hypotensive, bradycardic, and hypnotic responses to alpha2-adrenergic agonists in

spinophilin-null mice are accompanied by increased G protein coupling to the alpha2A-adrenergic receptor. MolPharmacol. 2010;78:279–86.
61. Muly EC, Smith Y, Allen P, Greengard P. Subcellular distribution of spinophilin immunolabeling in primate prefrontal cortex: localization to and within dendritic spines. J Comp Neurol. 2004;469:185–97.
62. Ben Zablah Y, Merovitch N, Jia Z. The role of ADF/Cofilin in synaptic physiology and Alzheimer's Disease. Front Cell Dev Biol. 2020;8:594998.
63. Chaaya N, Battle AR, Johnson LR. An update on contextual fear memory mechanisms: Transition between Amygdala and Hippocampus. Neurosci Biobehav Rev. 2018;92:43–54.
64. Wang Y, Dong Q, Xu XF, Feng X, Xin J, Wang DD, et al. Phosphorylation of cofilin regulates extinction of conditioned aversive memory via AMPAR trafficking. J Neurosci. 2013;33:6423–33.
65. Phillips RG, LeDoux JE. Differential contribution of amygdala and hippocampus to cued and contextual fear conditioning. Behav Neurosci. 1992;106:274–85.
66. Alvarez VA, Sabatini BL. Anatomical and physiological plasticity of dendritic spines. Annu Rev Neurosci. 2007;30:79–97.
67. Kasai H, Fukuda M, Watanabe S, Hayashi-Takagi A, Noguchi J. Structural dynamics of dendritic spines in memory and cognition. Trends Neurosci. 2010;33:121–9.
68. Bhatt DH, Zhang S, Gan WB. Dendritic spine dynamics. Annu Rev Physiol. 2009; 71:261–82.
69. Lynch G, Rex CS, Chen LY, Gall CM. The substrates of memory: defects, treatments, and enhancement. Eur J Pharm. 2008;585:2–13.
70. Richman JG, Brady AE, Wang Q, Hensel JL, Colbran RJ, Limbird LE. Agonist-regulated Interaction between alpha 2-Adrenergic Receptors and Spinophilin. J Biol Chem. 2001;276:15003–8.
71. Gilsbach R, Roser C, Beetz N, Brede M, Hadamek K, Haubold M, et al. Genetic dissection of alpha2-adrenoceptor functions in adrenergic versus nonadrenergic cells. Mol Pharm. 2009;75:1160–70.
72. Wang M, Ramos BP, Paspalas CD, Shu Y, Simen A, Duque A, et al. Alpha2A-adrenoceptors strengthen working memory networks by inhibiting cAMP-HCN channel signaling in prefrontal cortex. Cell 2007;129:397–410.
73. Harris NA, Isaac AT, Gunther A, Merkel K, Melchior J, Xu M, et al. Dorsal BNST alpha2A-adrenergic receptors produce HCN-dependent excitatory actions that initiate anxiogenic behaviors. J Neurosci. 2018;38:8922–42.
74. Kenakin T. Agonist-receptor efficacy. II. Agonist trafficking of receptor signals. Trends PharmacolSci. 1995;16:232–8.
75. Zhou L, Bohn LM. Functional selectivity of GPCR signaling in animals. Curr Opin Cell Biol. 2014;27:102–8.
76. Fernandez TJ, De Maria M, Lobingier BT. A cellular perspective of bias at G protein-coupled receptors. Protein Sci. 2020;29:1345–54.
77. Qu L, Zhou Q, Xu Y, Guo Y, Chen X, Yao D, et al. Structural basis of the diversity of adrenergic receptors. Cell Rep. 2019;29:2929–35.e2924.
78. Romeo I, Vallarino G, Turrini F, Roggeri A, Olivero G, Boggia R, et al. Presynaptic release-regulating alpha2 autoreceptors: potential molecular target for ellagic acid nutraceutical properties. Antioxidants. 2021;10:1759.

ACKNOWLEDGEMENTS

This works is funded by NIMH/NIH grant MH081917 (QW).

AUTHOR CONTRIBUTIONS

QW, KJ, NL, XL conceived, designed and/or planed experiments; SS, HR, YC, CC, HW, SL performed behavioral, biochemical, cell biological and/or pharmacological experiments; SZ and CA performed in-silico modeling study, QW, KJ, SS, YC, NL analyzed the data, QW, KJ, SS, CC, XL prepared manuscript.

COMPETING INTERESTS

The authors declare no competing interests.

ADDITIONAL INFORMATION

Supplementary information The online version contains supplementary material available at https://doi.org/10.1038/s41380-022-01851-w.

Correspondence and requests for materials should be addressed to Qin Wang.

Reprints and permission information is available at http://www.nature.com/reprints

Publisher's note Springer Nature remains neutral with regard to jurisdictional claims in published maps and institutional affiliations.